IOWA STATE UNIVERSITY
Digital Repository

Mechanical Engineering Publications | Mechanical Engineering

2018

Charts based on big data from fluid dynamics simulations provide a simple tool to estimate how far from its source a specific blood stain can be found

Daniel Attinger
Iowa State University, attinger@iastate.edu

Follow this and additional works at: https://lib.dr.iastate.edu/me_pubs

Part of the Engineering Physics Commons, Fluid Dynamics Commons, and the Medical Jurisprudence Commons

The complete bibliographic information for this item can be found at https://lib.dr.iastate.edu/me_pubs/309. For information on how to cite this item, please visit http://lib.dr.iastate.edu/howtocite.html.

This Article is brought to you for free and open access by the Mechanical Engineering at Iowa State University Digital Repository. It has been accepted for inclusion in Mechanical Engineering Publications by an authorized administrator of Iowa State University Digital Repository. For more information, please contact digirep@iastate.edu.

Charts based on big data from fluid dynamics simulations provide a simple tool to estimate how far from its source a specific blood stain can be found

Abstract
The bloodstain pattern analyst sometimes has to judge if a given stain could originate from a specific location. A wide range of values of the maximum distance that a blood drop can travel have been reported from experiments, ranging from less than one meter to more than 10 meter. Here we formulate the problem in a fluid dynamics and big data framework. The fluid dynamics is solved with Newton's classical equation of motion coupled with well-established models for the gravity and drag forces that bend the trajectories of drops. The parameters screened are the drop size, initial velocity and launch angle, as well as the height of a blood source and the ceiling height. Combining a wide range of values of those five parameter commended the performance of more than 4.5 million fluid dynamic simulations. Results of those simulations have been searched and mined for additional parameters directly measurable on a crime scene, such as the stain size and stain ellipticity. The results are presented in simple charts. Those charts are easy to use, and do not require any knowledge of fluid dynamics from the analyst.

Disciplines
Engineering Physics | Fluid Dynamics | Medical Jurisprudence

Comments
This manuscript based on presentation of D. Attinger at 1st "IABPA (International Association of Bloodstain Pattern Analysts) Congresso International de Analistas de Patrones de Manchas de Sangre," June 27-28, 2018, in Buenos Aires, Argentina. Presentation entitled "Determinacion de la distancia maxima de viaje de una gota de sangre" Posted with permission.

This article is available at Iowa State University Digital Repository: https://lib.dr.iastate.edu/me_pubs/309

Charts based on big data from fluid dynamics simulations provide a simple tool to estimate how far from its source a specific blood stain can be found

Daniel Attinger

Iowa State University, Mechanical Engineering Department, Ames IA 50010, USA

Charts based on big data from fluid dynamics simulations provide a simple tool to estimate how far from its source a specific blood stain can be found

Abstract

The bloodstain pattern analyst sometimes has to judge if a given stain could originate from a specific location. A wide range of values of the maximum distance that a blood drop can travel have been reported from experiments, ranging from less than one meter to more than 10 meter. Here we formulate the problem in a fluid dynamics and big data framework. The fluid dynamics is solved with Newton's classical equation of motion coupled with well-established models for the gravity and drag forces that bend the trajectories of drops. The parameters screened are the drop size, initial velocity and launch angle, as well as the height of a blood source and the ceiling height. Combining a wide range of values of those five parameter commended the performance of more than 4.5 million fluid dynamic simulations. Results of those simulations have been searched and mined for additional parameters directly measurable on a crime scene, such as the stain size and stain ellipticity. The results are presented in simple charts. Those charts are easy to use, and do not require any knowledge of fluid dynamics from the analyst.

Introduction

There has been an ambiance of mistrust between academic researchers and forensic practitioners. Leading scientific journals have criticized methods[1, 2] and results in forensics [3-7] . In 2009 [8], the National Research Council, the highest body of scientists in USA, harshly criticized the scientific basis of forensic sciences, including BPA. Forensic researchers mentioned that the applied nature of forensics could be better acknowledged [9, 10] in those criticisms. A way to improve the state of forensic sciences is to fund related fundamental research [11], as the US National Institute of Justice has been doing in BPA. Indeed, fundamental research in BPA has recently delivered new perspectives and augmented the science base. For instance, a method to infer the fall height of a dripping drop was designed based on a fluid dynamics analysis of the occurrence and abundance of spines [12]- which are pointy deformation at the periphery of a stain. The differences in size distribution between spatters from gunshot and those from beatings have been described quantitatively [13]. Uncertainties related to fluid dynamic conditions on the determination of the impact angle from stain inspection have been investigated quantitatively [14]. Quantitative differences have been identified between spatter drops on fabrics and their transfer onto fabrics by contact [15]. The fate of a dripping drop was characterized as a function of the impact conditions, with respect to spreading on various target materials [16]. Quantitative measurements were made of the wicking, rotation and deformation of stains caused by fabrics [17]. Fluid dynamic models of the atomization of blood have been formulated and tested against backward [18] and forward [19] gunshot spatters. Medium to large datasets of blood spatters [20] have been made available, in high resolution, to the scientific community for the purpose of testing methods and data. High Speed videos describing the multiple physical phenomena related to BPA were produced [21], and quantitative measurements thereof have estimated the velocities and drop sizes resulting from gunshot atomization [22]. State of the art image processing methods [23] were described to quantitatively describe the multiple stains (more than 40,000 in some gunshot spatters). Automated classification methods were

developed [24] to discriminate between two mechanisms causing blood spatters. Also, blood is a complex fluid with properties that are not yet fully known. Its properties have been further characterized in terms of storage life [25] and extensional viscosity [26]. Blood substitutes have been proposed[27] to facilitate teaching. Trajectory models accounting for the effect of drag and gravity on drops were formulated and calibrated [28, 29]. Many of the rationale for these research efforts can be justified [30] by the multiple and natural connections between fluid dynamics and bloodstain pattern analysis.

Despite the above acceleration of research, it is not clear to the author if any of the above efforts has resulted in novel methods currently used in the field. It certainly takes time to vet academic progresses and to package these into useable tools. It is also a complex task to change an industry. For instance, airline pilots still communicate with control towers using low quality analog radio, despite more advanced digital systems like FANS [31], which have been under development since at least the 1990s. Those digital systems provide clear voice quality with written transcription. Importantly, new forensic methods must be robust, easy to use, offer a significant improvement over the state of the art, with other desirable requirements such as a known uncertainty and error.

Here we address a practical problem relevant to BPA with a set of charts that can be used without knowledge of the complex underlying physics. The fluid dynamics is indeed packaged in a large data set of millions of simulation results, the useful results of which are provided as simple charts. The practical problem is as follows. The bloodstain pattern analyst sometimes has to assess if a given blood stain could have originated from a given location at a crime scene. Thus arises the question of how far a blood drop can travel.

This question has been addressed experimentally in several studies. The location of stains furthest away (horizontally) from a blood source has been measured in studies of gunshots, where various guns, ammunition, settings and blood source have been used. Examples of blood sources include calves heads [32], a human cadaver filled with blood [33], foams or sponges soaked in blood [13, 34], or cavities filled with blood [19]. Some experimental results of bloodstain spatters were selected for comparison with theoretical and numerical studies, and the maximum experimental distances were 70cm [35] for backspatters and 4 meter for forward spatter [19]. An anonymous literature review in the 2007 newsletter of the International Association of Bloodstain Pattern Analyst [36] mentions 12 references for “distance that backspatter travels”. Depending on the study cited, the maximum distances given are between 30cm ($\cong$ 1 foot) and 6.5 feet ($\cong$ 198cm). It is important to mention that not every one of the work cited [37-42] was focused on the same single issue of how far on drop can travel. Some studies were focused on how far sub mm-stains would travel [43], while some other were focused on the presence or not of stains on the hands holding the gun [41]. At the 2018 IABPA conference, the presentation “Slugger Slaying Caught on Tape” by John Bockrath and Ray Lugo describe a beating in a Walmart department store [44]. The beating was recorded by the surveillance cameras which offers a unique and gruesome piece of data. The victim was on the floor and did not move; their head was destroyed by repeated assaults with a baseball bat, and the furthest stain was found 33 feet ($\cong$ 10.1 m) away from the region of origin of the spatter, which as far as we know is the world record.

Note that there is little standardization in the above studies with respect to the blood (human or animal), its hematocrit (known or unknown), its temperature (ambient or heated), its container and the height of the blood source over the floor. The present theoretical work solves the problem in a general manner, with clearly stated assumptions. Comparisons with experimental data are consistent with the theory. Below, the presentation of the study starts with a brief presentation of the theoretical framework, which leads to results and their discussions, followed by a thorough description of the methods used to obtain those results.

Theoretical question and framework

The theoretical question addressed in this manuscript is as represented in Figure 1: "A blood source at height *h* over a horizontal floor, in a room with ceiling at height H, generates drops with a broad and realistic range of diameters, initial velocities and launch angles. How far from the blood source will the corresponding stains be?

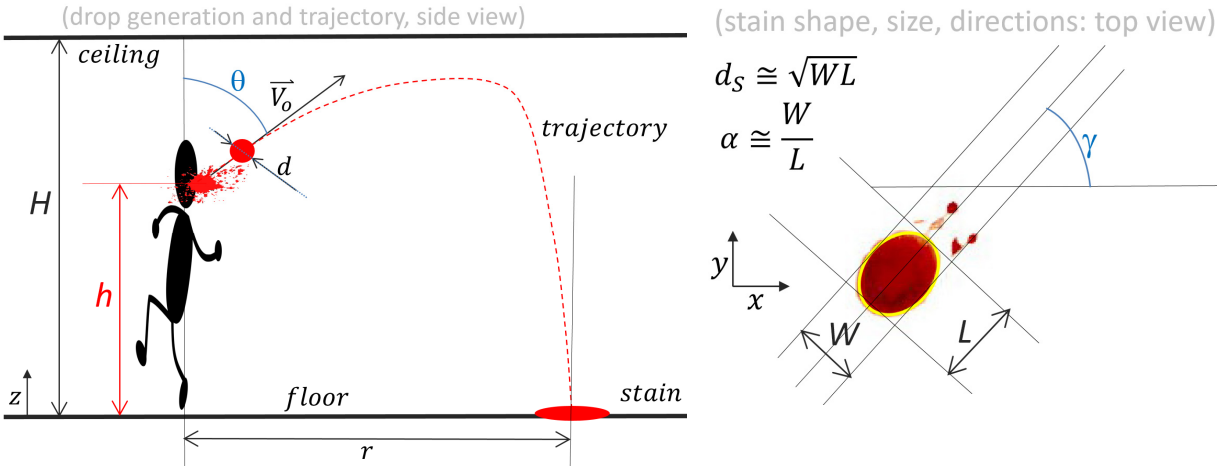

Figure 1: representation of the problem at hand: 'How far can a blood drop travel from a blood source?". The side view describes the controlling variables of the forward problems: two heights (origin and ceiling), the initial velocity and launch angle θ, as well as the drop diameter. The top view shows how the main direction of the stain determines the directional angle γ, and how the width W and length L of an ellipse fitted on the stain are used to determine impact angle α and equivalent diameter d_S. We use equivalent diameter because it is simpler to use than area for the analyst. In the case of a round stain, the equivalent diameter is simply the diameter of the stain.

Note that this theoretical question above correspond to a physical and deterministic problem. By deterministic we mean a problem proceeding forward in time, from well-known known initial conditions. Questions asked to forensic investigators are never that simple, as those questions are rather reconstruction problems. Indeed, in a bloody crime or accident, little is known about velocities and drop sizes. The available evidence is one or several stains, or patterns thereof, on a given target surface. The investigator can measure their orientations, sizes and shapes. The question asked by the bloodstain pattern analyst is thus not the deterministic question above ("How far a blood drop can travel?"), but the slightly different question: "Considering a stain, what is the ensemble of locations in

space it could have originated?" This reconstruction question could be solved by proceeding backward in time from impact conditions inferred from stain inspection.

To answer the two above questions, we design and perform numerical simulations to calculate a data set of drop trajectories, screening a wide range of initial velocities and drop sizes, of room dimensions and of height of the blood source. The range of parameters is presented in Table 1.

Parameter, symbol, unit	**Number of values**	**[minimum, increment, maximum – separated by commas] or [list of values separated by space]**
Ceiling height, H, m	9 **(1)**	[2.5 **2.75** 3 3.25 3.5 3.75 4 4.25 4.5]
Blood source height, h, m	19 **(1)**	[0 10 20 30 40 50 60 70 80 90 100 110 120 130 140 150 **160** 170 180]
Launch angle θ, degree	28 (**15**)	[**0** 5 **10** 15 **20** **25** 27.5 **30** 32.5 **35** 37.5 **40** 42.5 **45** 47.5 **50** 52.5 **55** 57.5 **60** 62.5 **65** 67.5 **70** 75 **80** 85 **90**]
Drop diameter, mm	29 **(12)**	[**0.033** **0.066** **0.1** 0.2 **0.3** 0.4 0.5 0.6 **0.7** 0.8 0.9 **1** 1.3. 1.6 **2** 2.3 2.6 **3** 3.3 3.6 **4** 4.5 **5** 5.5 6 **7** 8 9 **10**]
Initial velocity, m/s	35 **(12)**	[**0.01** 0.015 0.02 0.03 0.04 **0.05** 0.075 **0.1** 0.25 **0.5** 0.75 **1** **2** 3 **4** 5 **7.5** **10** 12.5 15 17.5 **20** 22.5 25 27.5 **30** 35 40 45 50 60 70 80 90 **100**]

Table 1: list of the discrete parameters used in the trajectory simulations. Total number of simulations considered in this manuscript is the product of each number of values: 4.86 million of simulations. A smaller set of parameters, in bold, is plotted in the example Figure 2.

Each trajectory is calculated by numerical integration of Newton's second law for a drop moving through the air, proceeding forward in time until the drop either hits the ceiling, the floor, or breaks up in flight. The calculation of the drag force is based on published models based on comparisons between experiments and simulations. The drag model considers that drops deform in flight, and the corresponding increase of drag. Information on stain ellipticity is estimated from the numerically calculated impact angle, and stain size is estimated from widely used spreading correlations. The resulting data set is relatively large, corresponding to about five millions of different trajectories. Numerical sorting and search of the data set is then performed to produce charts of interest for forensic reconstruction. Those charts are presented in the results section, with clear instructions on how to use these and on the underlying hypotheses. Results of the theoretical simulations are finally compared with several experiments documented in the BPA literature, as well as a limited set of gunshot spatter experiments performed in the context of this work. Details of the simulations and methods are provided in a later, specific section.

Results and Discussion

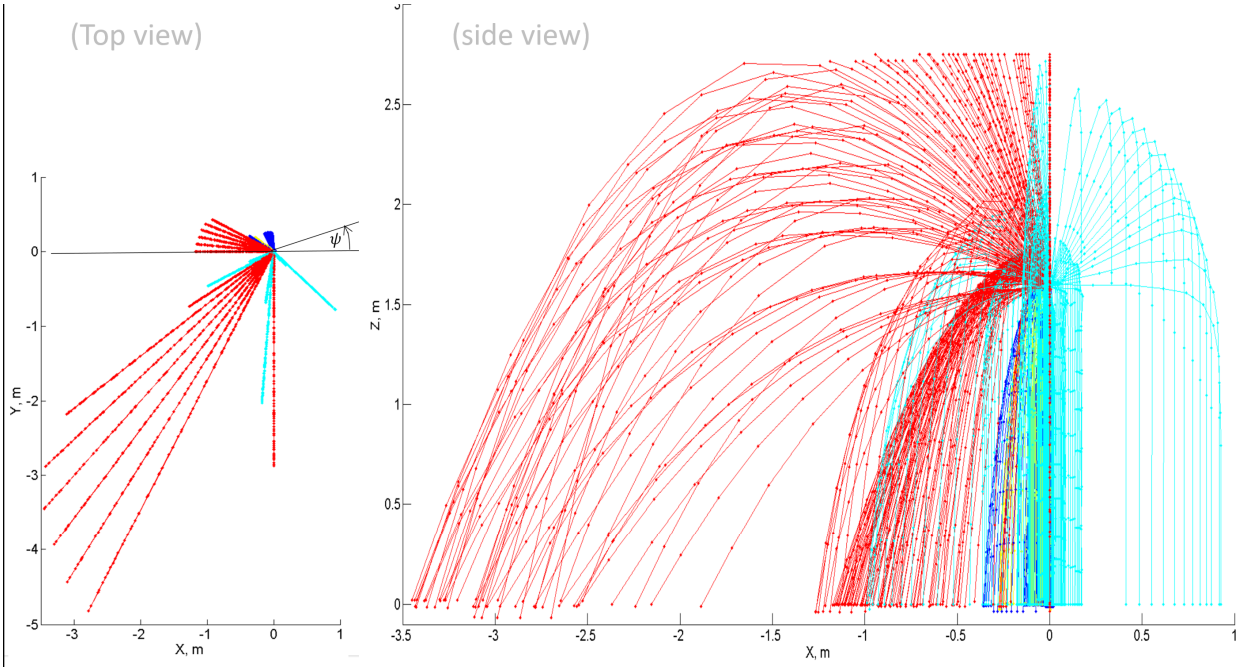

Figure 2: 3D geometry of 2160 simulated trajectories, corresponding to less than 0.5 per mil of all the simulations performed. Colors inform on the initial and boundary conditions, which are those of the bolded parameters in Table 1. Red means large (d>1mm) and fast (V0>1m/s) drops; blue, large and slow; cyan small and fast; yellow small and slow. Yellow trajectories are barely visible because small and slow drops do not travel further than a few cm. While all the simulations are calculated in the two-dimensional plane X-Z, the trajectories are plotted with an arbitrary rotation around the vertical axis, set by angle $\in [0,360°]$, to reduce overlap and improve visibility.

In figure 2, the ceiling height is 2.75 m (~9 feet) and some red trajectories are seen to hit and stop and the ceiling. Note also the small and fast drops that (cyan) ultimately fall almost vertically to the floor (on the right): those drops descend at terminal velocity, and will create round stains that have lost any directionality.

Numerical results

Several numerical results of interest are provided. Figure 3 describes the maximum distance that a stain on the floor can be found away from a blood source, as a function of the stain size and shape. This maximum distance is larger than 7 meter, and is reached by stains with equivalent diameters in the 10-50mm range. The size of the stain is described by its equivalent diameter, $d_S = \sqrt{\frac{4A}{\pi}}$, which is approximately equal to $\sqrt{WL}$, as represented in Figure 1, right. Above, the symbols *A, W* and *L* stand for the area of the stain, and the width and length of an ellipse fitted to the stain, respectively. The shape of the stain is defined by the ellipticity of a best-fitted ellipse $\varepsilon = \frac{W}{L}$. Other variables illustrated in Figure 1 such as ceiling height, height of blood source, drop diameter and drop velocity could take any combination of values of Table 1. On the left of the plot, the accumulation of vertical contours describe the fact that stains with sub-mm size do not travel

far from the source, which is consistent with experimental observations that the “mist’ produced by backspatter does not travel further than a few feet [36]. Since no constraints were set on the height of the blood source, of the ceiling, nor on the initial velocity, it is possible that some results for specific values of ceiling height and source height are smaller than in Figure 3. Such specific cases are studied in figures Figure 4 and Figure 5.

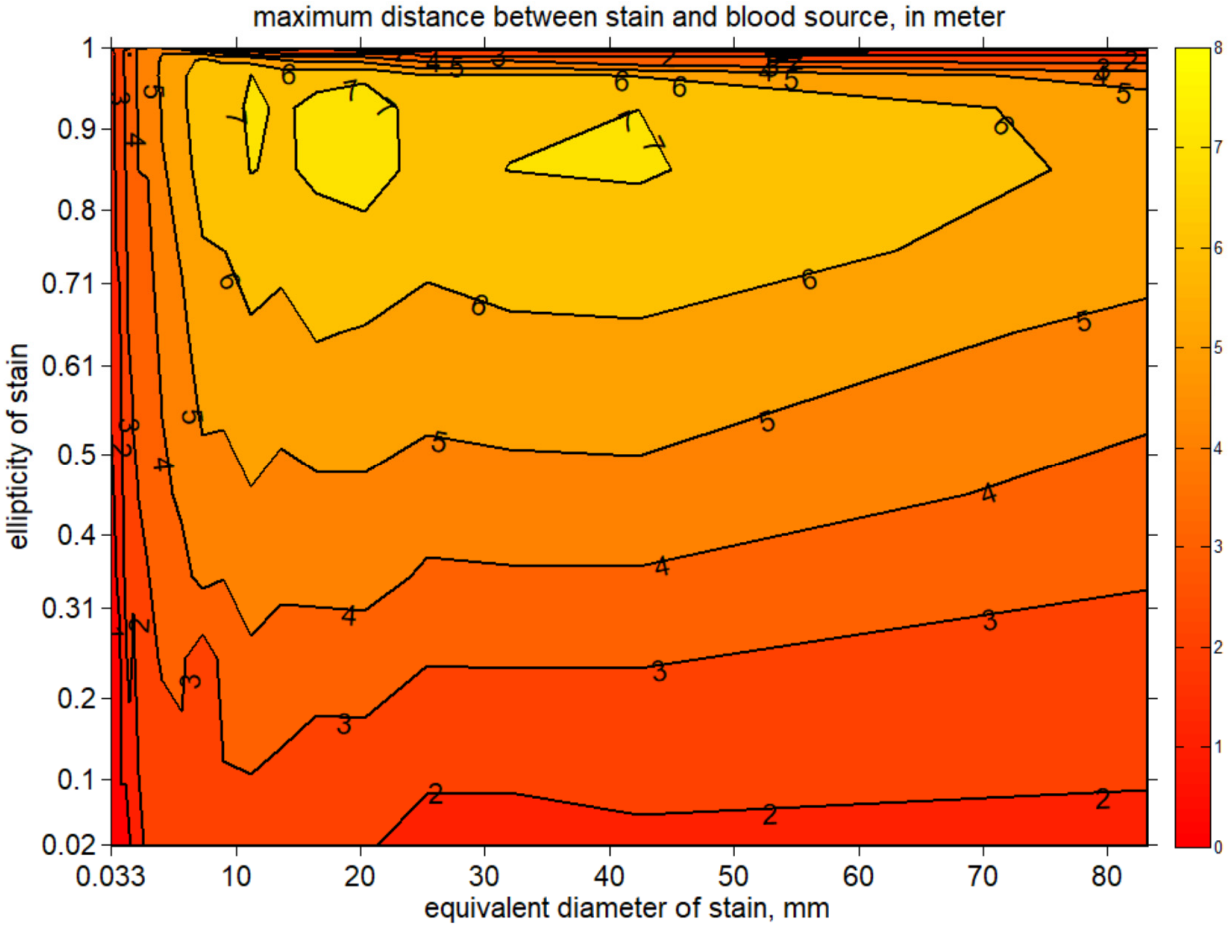

Figure 3: Maximum horizontal distance, in meter, between a stain on the floor of a crime scene and its blood source, as a function of the stain size and shape. Data is generated assuming that the height of the blood source, of the ceiling, the initial velocity and the launch angle, can take any combination of values listed in Table 1.

It is also possible to screen the numerical results for more specific situations, to obtain even more precise answers. For instance, let us assume that the position of the blood source is known, from, e.g. wound evidence or concurring testimony. This limits the range of source heights, as shown with the model photographs in Figure 4. Heights corresponding to the three positions (lying on the floor, sitting, standing) are listed in the figure, in an exclusive way, assuming a height range that only corresponds to on given position.

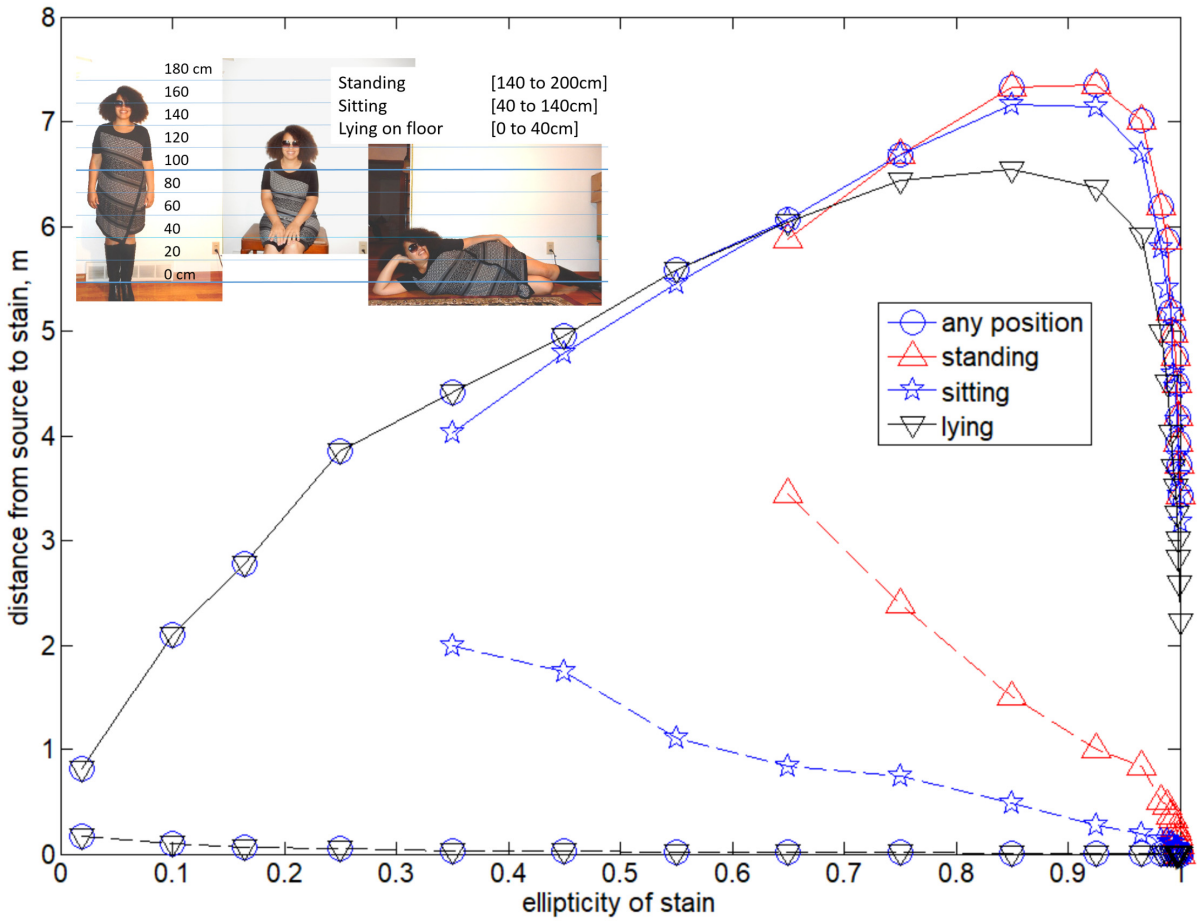

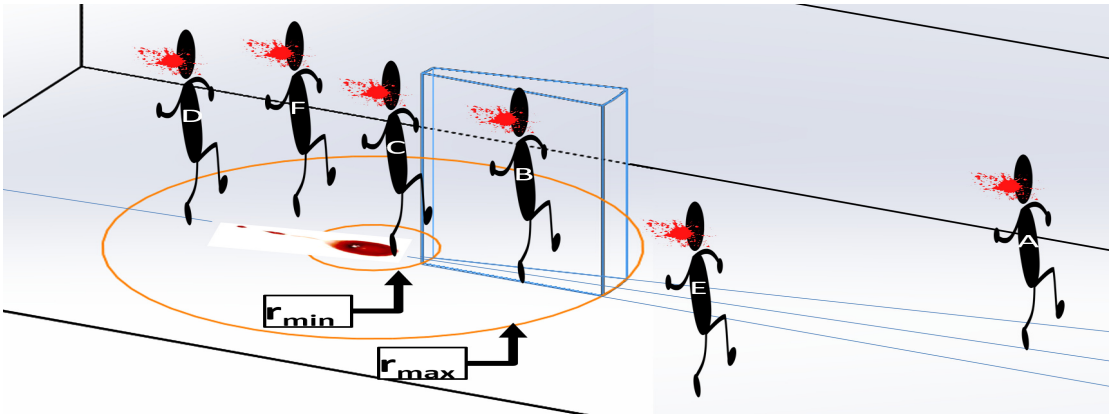

Figure 4: (Top) Distance in meter between a stain and its blood source as a function of the drop ellipticity and the position of the victim. Minimum distance is hatched, maximum, continuous. Illustration of the additional information on source height if the position of the victim is known. Here the positions (standing, sitting or lying on the floor) are described in an exclusive manner in terms of the associated heights. Model participation is for illustration only; model does not endorse the methods or results presented in this manuscript. Data generated assuming that the height of the ceiling, and the initial velocity, drop size and the launch angle, can take any combination of values listed in Table 1. Example (Bottom) of use of the top chart: among possible positions A-F, only positions B is compatible with the shape, orientation of the stain and blood source location.

Curves in Figure 4 (top) describes the maximum and minimum horizontal distances between a stain and its source, with respective hatched and continuous color lines, as a function of the position of the source and the ellipticity of the stain. For instance, if the blood is known to originate from a standing person, and the measured ellipticity of the stain is 0.7, the red curves provide the maximum and minimum horizontal distances are $r_{min} \cong 3m;\ r_{max} \cong 6m$. Interestingly, no stain with ellipticity less than 0.5 can come from a standing person as a source; and a sitting source also is not compatible with ellipticity less than 0.3. Figure 4 (bottom) explains how to combine the chart in Figure 4 and known BPA knowledge to discriminate among possible and impossible location of the victim: locations E and A are impossible because their horizontal distance to the stain is larger than r_{max}; location C is impossible because its horizontal distance to the stain is smaller than r_{min}; location F and E are not aligned with the main direction of the stain, thus impossible; location D is aligned with the main direction and within the correct distance, but the presence of the splashing features (also called wave cast-off) indicate that the drop flew from the opposite side of the stain, the side of location B. Thus only location B is compatible with the stain of interest. Note that we assume a specific uncertainty on the directionality of the stain, as Camana does [45], and this uncertainty is represented by the thickness of the wedge. For persons with widely different heights or figure than the model, in-situ measurements with a model of similar size as the person of interest remain necessary.

The problem in Figure 4 can also be solved by considering the available information of the stain size. Results in that case are reported with two plots in Figure 5, one for the maximum and one for the minimum horizontal distance that a stain can be found from its blood source. In the specific case of a stain with equivalent diameter of 20mm, the use of Figure 5 determines the minimum distance as larger than 3.3m, while Figure 4 determines the distance as larger than 3m – without using information on the stain size. Thus, the additional information on stain size can reduce the uncertainty on the location of the blood source in specific cases.

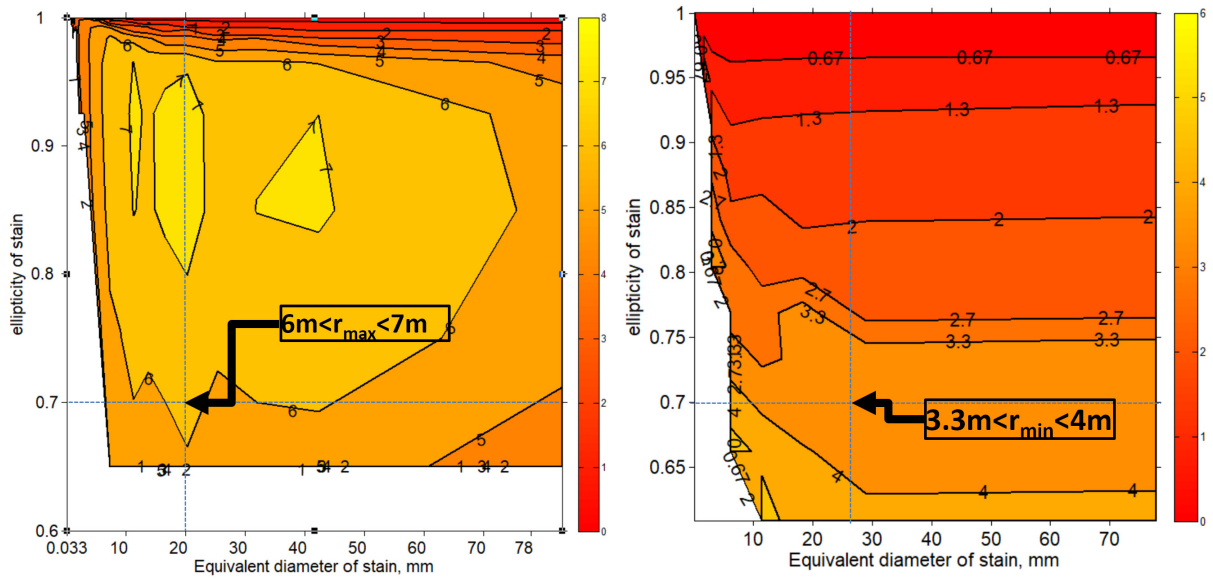

Figure 5: Maximum (left) and minimum (right) horizontal distance, in meter, between a stain and its blood source, as a function of the drop size and velocity. Source height is that of a standing person. Ceiling height, drop size, launch angle and drop velocity can take any value in Table 1. Results indicated by the bold arrow correspond to the maximum and minimum radii of the circles in Figure 4 bottom.

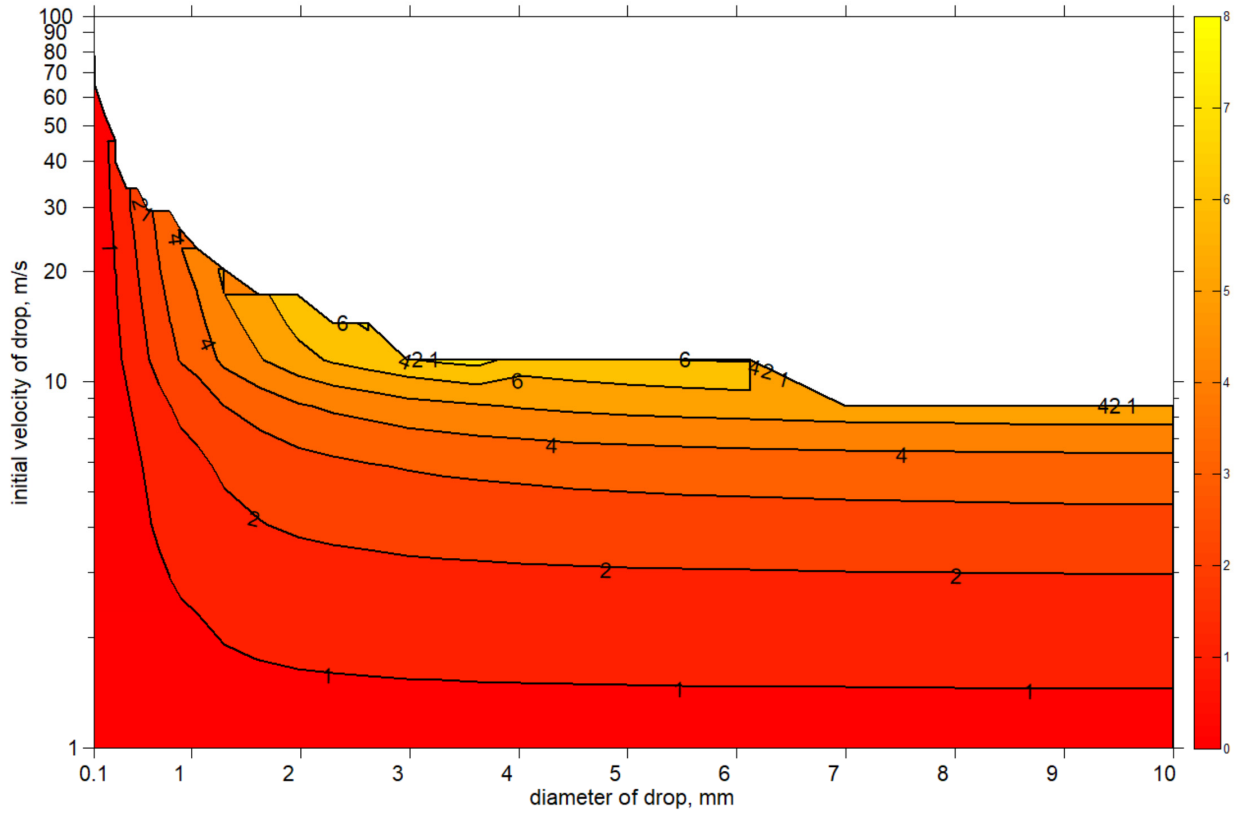

Figure 6: Horizontal distance between a stain and a blood source, as a function of the initial velocity of the drop and the diameter of the drop. Regions without color correspond to aerobreakup. Data generated assuming that the height of the blood source, of the ceiling, and launch angle can take any combination of values listed in Table 1.

Figure 6 has no practical use but informs on several aspects of the fluid dynamics at hand. It plots the same maximum distance between stain and blood source as Figure 3, however as a function of the initial drop size and drop velocity. Figure 6 is not directly useful on a crime scene, because drop size and initial velocities are unknown. While past literature has associated typical drop sizes and velocities to specific events such as beatings and gunshot, recent measurements [22] with a technique called Particle Image Velocimetry have shown that the single same atomization mechanism, a gunshot by Laber et al. [21], would generate a wide range of drops sizes and initial velocities. Interestingly, the drops that travel the farthest are those with average size ($d \in [2mm - 6mm]$ and average velocity ($V \cong 14m/s$). Faster drops corresponds to the white region in Figure 5 where drag overcomes surface tension and the drop explodes in flight. Technically this corresponds to a situation where the Weber number reaches values larger than the critical value for breakup in flight. Smaller drops suffer from a disproportionally strong drag, with respect to their inertia, and do not travel much – less than 1 meter for drops smaller thank 500 micrometer. Larger drops can only be thrown at velocities below 10m/s, to avoid explosions in flight. This explains that larger drops cannot travel as far as those with average size. Charts like Figure 6 summarize millions of numerical simulations and allow to see through various aspects of the physics of the problem, in a different way than via experiments.

In interpreting the numerical results, it is important to keep in mind the assumptions underlying the calculations presented here.

a) Deformation of drops during flight under the effect of drag forces [46] is considered. If the Weber number, which here quantifies the effect of drag over surface tension forces, becomes larger than 13 along the trajectory, the drop breaks up and no results of maximum distance are returned.
b) Blood properties are same as those of swine blood at 22°C [47].
c) In case of gunshot spatters, muzzle gases do not modify the drop trajectories.
d) Each drop travels independently from any other. The 'bird formation flight' effect in [18] is thus neglected. Consideration of this drag reduction effect might increase the maximum distance between drop and source, especially for situations where the launch angle is within a narrow range – like jets in e.g., arterial gushing.
e) Stains are produced on the horizontal floor. Any stain produced on a vertical wall might have traveled a smaller distance.
f) The spreading of stains on the target non-absorbing surface is similar to that measured on smooth cardstock [48].
g) The stain ellipticity is a simple function of the impact angle, shown in Figure 1, for any fluid dynamic conditions.

Experimental results: While this study is essentially theoretical, experiments were also performed. The blood source was a cavity filled with blood, similar to the one used described in [19], set at height 1.3m. The blood source was hit by a full metal jacket bullet shot with either a rifle or a handgun. No attempt was made to screen the muzzle gases, although the gun was held relatively far from the blood source, about 250 cm. The floor of the shooting range was covered with 5 lines of 36'' butcher paper, corresponding to width of about 4.55 m (180 inch) and length in the direction of the bullet path of about 10 meter. The ceiling of the shooting range was measured as 260cm. The most remote stains were circled with pencil on the butcher papers, which have been preserved. The horizontal distance between the most remote blood stain and the blood source was recorded. Two experiments were made with the handgun, and one with the rifle. Bullets and guns are described in Table 2.

Gun label	**description**
Rock River Arms rifle .223''	LAR-15 16'' barrel length M-4, .223 caliber (5.66 mm), with Yankee Hill YHM Phantom 223 suppressor
S&W 9 mm	Smith and Wesson M&P Caliber 9mm, with 4.25'' barrel length.

Bullet label (tip shape)	**Velocity, m/s**	**Full description**	**Picture**
AE223 (pointy)	~987	FMJ rifle rounds, Federal Ammunition American Eagle #AE223, bullet mass 55 grain, .223 rem.	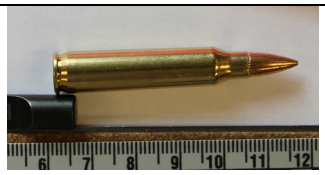
AE9FP (flat)	285	FMJ flat nose handgun ammunition, Federal Ammunition American Eagle #AE9FP, 147 grain, 9 mm.	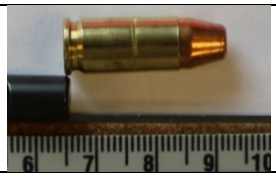

Table 2: guns and bullets used in the experiments, with #manufacturer number. Velocities are either as per manufacturer data (and preceded with the symbol "~") or measured with a chronograph at the shooting range. The grain is a measure of mass, and can be converted to SI units as 1 grain ≅ 64.8 mg. Pictured ruler has cm units.

Temperature in the shooting range was 15°C and the hematocrit of the pig's blood used was 39%. Maximum distances measured were 3.92 m for the rifle and 5.45 meter for the handgun. Note that those experiments were not as extensive as many reported in the above literature review, but were produced within a larger effort focused on creating a data base of freely-available high-resolution spatters [20]. Considering our experiment and the above literature review, maximum distances reported experimentally between a blood stain and its source varies between 30cm and 10 meter. Comparison between experimental and numerical results is shown in Figure 7.

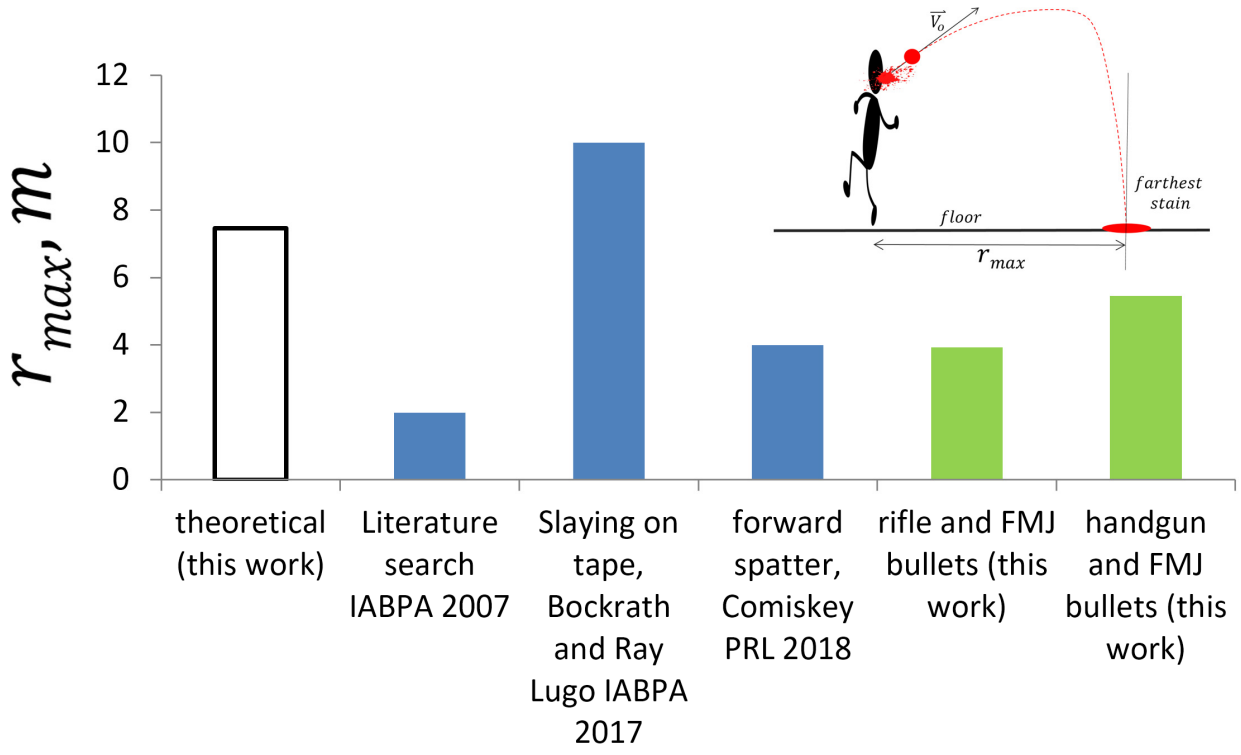

Figure 7: Reported maximum horizontal distance between stains and blood source, r_{max}. Comparison of simulations in this work and various experiments in this work and in the published literature [19, 36, 44].

Reported experimental distances are smaller than the maximum predicted by our simulations in four out of five occurrences. This is to be expected because the numerical simulations correspond to every possible combination of drop size, velocity, launch angle, while any experiments will only produce a subset of those combinations – although gunshot backspatters have been shown to produce 40,000 stains [49]. One reported experimental result is larger than the theoretical maximum, by about 2 meter. This is unexpected, and the author remembers addressing the issue in the questions following the oral presentation [44]. Possibly, one or several assumptions of the numerical simulations presented here need to be revisited. The speaker hinted at the fact that the stain was possibly not pure blood but rather brain matter. Indeed tissues such as brain matter behave differently than fluids, because they have internal structure that maintain their cohesion. They behave differently in the way fragments are created upon impact; also, flying chunks of brain matter deform less than blood drops and are less likely to break up because of drag forces. There is certainly a lot more physics to uncover in the gruesome world of bloodstain patterns.

Methods

There is a wide body of engineering literature describing the trajectories of flying drops, in relation to e.g. inkjet printing [47] or raindrops [50]. Thus simulations such as those presented here do not present specific difficulties beyond the challenge of running 4 millions of these within a reasonable amount of time. The simulation equations and framework are described below.

The trajectories of flying drops are described with an equation of motion based on Newton's law:

$$m_d \frac{d\vec{V}}{dt} = m_d\overrightarrow{g} - \overrightarrow{F_D}. \quad (1)$$

Above, $m_d, t, V, \overrightarrow{g}, \overrightarrow{F_D}$ are the drop mass, time, drop velocity, gravity acceleration and drag force, respectively. It is assumed that the air is quiescent, and that the interactions between drops are negligible Lift forces are also neglected – those would matter if the drop spins and such information is unavailable at the time of reconstruction.

To calculate the equation of motion (1), it is necessary to estimate the drag caused by the air on the travelling droplet. The drag force is defined as in [47]

$$\overrightarrow{F_D} = \rho_a C_D \frac{A_d}{2} \vec{V} V , \quad (2)$$

where $\rho_a, A_d, V \text{ and } \vec{V}$ are the air density, the cross-sectional area of the undeformed droplet ($A_d=\pi d^2/4$), the velocity magnitude and velocity vector of the droplet, respectively. The dimensionless parameter C_D is a drag coefficient for isolated spherical particle, modified to account for the particle deformation that occurs at intermediate Weber number. Indeed, when the Weber number becomes larger than one, the drop becomes oblate, with a ratio of the largest diameter to the smallest that can be as high as 5. At higher drag, the drop has been observed to explode in flight, and those trajectories are excluded from the simulation. The drag coefficient has been validated against a wide body of experimental studies reviewed and synthetized by Loth [51], and is expressed as.

$$C_D = C_{D,sphere} + \Delta C_D \cdot \left(C_{D,deformed} - C_{D,sphere} \right). \qquad 0 \le We \le 13,400 \le Re \le 7000 \quad (3)$$

In the above equation, $\Delta C_D = f(We_a, Re_a)$ is explicitly provided in [51] as a fit from experiments with drops of various fluids in air by Reinhart [52]. The Reynolds and Weber numbers are based

on air as the fluid. The drag coefficient for an isolated spherical particle is an extension for intermediate Reynolds numbers of the widely-used Clift-Gauvin [53] drag coefficient as

$$C_{D,sphere} = \left[\frac{24}{\mathrm{Re}}\left(1+0.15\,\mathrm{Re}^{0.687}\right)\right] + \frac{0.42}{1+42500/\mathrm{Re}^{1.16}} \qquad 0.1 \le \mathrm{Re} \le 2\times10^{5}, \tag{4}$$

and the drag coefficient corresponding to the maximum deformation is an empirical relation by Clift et al. [53]

$$C_{D,deformed} = \frac{8}{3} + \left[\frac{24}{\mathrm{Re}}\left(\frac{2+3\mu^{*}}{3+3\mu^{*}}\right)\right] , \tag{5}$$

with $\mu^{*}$the ratio of the dynamic viscosities of the blood and the air. Comparison between the drag coefficient used in this study and the one correlated on experiments by Vargas et al. [50] showed no significant difference in the trajectories.

Once the drop hits the ceiling or the floor, the angle between its velocity and the target surface is used to estimate the stain ellipticity and produce plots such as Figure 3 and Figure 4. To produce charts such as Figure 5, and additional a relation is needed to estimate drop spreading and the size of the resulting stain. For oblique impact, Adam [54] has shown that a correlation exist between normal impact velocity and drop spreading. This correlation can be expressed [55] in the way proposed by Bousfield and Scheller [54, 56],

$$\beta = W/D = a(Re_N^2 Oh)^b. \tag{6}$$

Above, β is the spread ratio expressing how much the drop spreads upon impact. It is defined as the ratio of stain width over initial drop diameter. The coefficients are specific to the impact surface, and here we use coefficients a=0.257 and b=0.235 [48], measured on smooth cardstock. Those correspond to a non-absorbing surface with average spreading, in the sense that drops would spread more on glass and less on plastic [48]. The Reynolds number $Re_N = \rho V_n d/\mu$ measures the ratio of the blood inertia normal to the impact surface to the viscous forces inside the drop, and the Ohnesorge number $Oh = \frac{\mu}{\sqrt{\rho d \sigma}}$ scales inertial with respect to the resisting viscous and surface tension forces. Symbols $\rho, \mu \; and \; \sigma$, are the density, viscosity, and surface tension of the blood drop, respectively, and *u* is the velocity component normal to the target. In the above numerical calculations and equations, the following values are used for the physical properties of air and blood: blood density $\rho = 1060$ kg/m^3; surface tension between blood and air σ = 59 mN/m; dynamic viscosity of blood μ =42cP; dynamic viscosity of air $\mu_a = 1.98$ x10-5 Pa·s; density of the air $\rho_a = 1.229$ kg/m3. The blood properties correspond to swine blood, considered an adequate substitute for human blood in BPA experiments, at temperature of 22°C and hematocrit of 45% [48]. The critical Weber number for drop breakup in flight is set to 13, consistently with extensive experimental studies by Hsiang and Faeth [57, 58].

The total number of simulations is the product of the numbers of each parameters in Table 1, p=9x19x28x27x35 simulations, which represents more than 4.5 million simulations. Simulations

were conducted using the scientific computing language MATLAB [59] version 2013b, which is reasonably fast at integrating ordinary differential equations and excellent at manipulating large amounts of numerical data. Simulations took about 48 hours on a 2016 workstation (Intel i7 CPU at 2.7GHz, with 32GB of RAM). Results and input parameters of the simulations, including trajectories as well as the fate of the drop, which either hit the ceiling, hit the floor, or exploded in flight, have been saved into a structured data file of 24 GB. Sorts and search operations with were then used to identify data suitable to be plotted.

Conclusion

A large dataset of more than four million of numerically calculated trajectories of blood drops is produced and mined to determine the maximum distance between a blood stain and the source of the blood. The governing equations are presented, and the simulation results depend on the following variables: drop size, drop initial velocity and launch angle, height of blood source and height of ceiling. The numerical results are presented as a set of charts that can be directly useful for the bloodstain pattern analyst. Results are presented using variables that are directly and easily observed on the crime scene, such as the stain size and its ellipticity. The packaging of complex physics into a tool that is simple to use and that does not require any knowledge of fluid dynamics is analog to a pregnancy test. Throw-away pregnancy tests packages complex chemistry and biology, even fluid dynamics, in a way that is easy to use and produce reliable results. As such, the “pregnancy test” approach presented in this work is worthy of pursuing to design tools for the BPA analyst, besides the classical approach which consists in teaching fluid dynamics to bloodstain pattern analysts. We would certainly recommend considering both approaches, considering that a typical university like Iowa State University or EPFL allocate more than 800 hours to teach basic fluid dynamics to their undergraduate students.

The author acknowledges financial support from the US National Institute of Justice (Grant No. 2017-DN-BX-0171). We acknowledge useful discussions with the Las Vegas Metro Police Department; contribution by Officer Darin van Rysvyk for the gunshot experiments and by John Polansky in specific aspects of the numerical integration of the ordinary differential equations; as well as the help of Ricky Faflak for the gunshot experiments and in drafting Figure 7.

Bibliography

[1] D. Kennedy, "Forensic science: Oxymoron?," *Science,* vol. 302, no. 5651, pp. 1625-1625, Dec 2003.

[2] I. E. Dror, "Biases in forensic experts," *Science,* vol. 360, no. 6386, pp. 243-243, Apr 2018.

[3] A. Cho, "Forensic science - Fingerprinting doesn't hold up as a science in court," *Science,* vol. 295, no. 5554, pp. 418-418, Jan 2002.

[4] A. Cho, "Forensic science - Judge reverses decision on fingerprint evidence," *Science,* vol. 295, no. 5563, pp. 2195-+, Mar 2002.

[5] K. Page, "Forensic science - Reformers aim to shake up British system," *Science,* vol. 301, no. 5633, pp. 579-580, Aug 2003.

[6] M. J. Saks and J. J. Koehler, "The coming paradigm shift in forensic identification science," *Science,* vol. 309, no. 5736, pp. 892-895, Aug 2005.

[7] R. Mejia, "Label the limits of forensic science," *Nature,* vol. 544, no. 7648, pp. 7-7, Apr 2017.

[8] "Strengthening Forensic Science in the United States: A Path Forward," Committee on Identifying the Needs of the Forensic Sciences Community, National Research Council (National Research Council. Washington, DC: The National Academies Press, 2009. doi:10.17226/12589.)2009.

[9] J. P. Polski, "The science behind forensic science," *Science,* vol. 304, no. 5669, pp. 389-389, Apr 2004.

[10] C. S. Palenik and S. J. Palenik, "Forensic science and academic science," *Science,* vol. 303, no. 5661, pp. 1136-1136, Feb 2004.

[11] M. Tibbett, "Step up funding to halt forensic folly," *Nature,* vol. 501, no. 7465, pp. 33-33, Sep 2013.

[12] L. Hulse-Smith, N. Z. Mehdizadeh, and S. Chandra, "Deducing drop size and impact velocity from circular bloodstains," *Journal of Forensic Sciences,* vol. 50, no. 1, pp. 54-63, 2005.

[13] S. Siu, J. Pender, F. Springer, F. Tulleners, and W. Ristenpart, "Quantitative Differentiation of Bloodstain Patterns Resulting from Gunshot and Blunt Force Impacts," (in eng), *J Forensic Sci,* Feb 10 2017.

[14] M. Lockard, "THE FLUID DYNAMICS OF DROPLET IMPACTS ON INCLINED SURFACES WITH APPLICATION TO FORENSIC BLOOD-SPATTER ANALYSIS," Mechanical Engineering, Georgia Tech, 2015.

[15] Y. Cho, F. Springer, F. A. Tulleners, and W. D. Ristenpart, "Quantitative bloodstain analysis: Differentiation of contact transfer patterns versus spatter patterns on fabric via microscopic inspection," *Forensic Science International,* vol. 249, pp. 233-240, Apr 2015.

[16] S. Kim, Y. Ma, P. Agrawal, and D. Attinger, "Corrigendum to “How important is it to consider target properties and hematocrit in bloodstain pattern analysis?” [FSI 266C (2016) 178–184]," *Forensic Science International,* vol. 287, p. 217, 2018/06/01/ 2018.

[17] P. Agrawal, L. Barnet, and D. Attinger, "Bloodstains on woven fabric: Simulations and experiments for quantifying the uncertainty on the impact and directional angles," *Forensic Science International,* vol. 278, pp. 240-252, 2017/09/01/ 2017.

[18] P. M. Comiskey, A. L. Yarin, and D. Attinger, "Hydrodynamics of back spatter by blunt bullet gunshot with a link to bloodstain pattern analysis," *Physical Review Fluids,* vol. 2, no. 7, p. 073906, 2017.

[19] P. M. Comiskey, A. L. Yarin, and D. Attinger, "Theoretical and experimental investigation of forward spatter of blood from a gunshot," *Physical Review Fluids,* vol. 3, no. 6, p. 063901, Jun 2018, Art. no. 063901.

[20] D. Attinger, Y. Liu, T. Bybee, and K. De Brabanter, "A data set of bloodstain patterns for teaching and research in bloodstain pattern analysis: Impact beating spatters," *Data in Brief,* vol. 18, pp. 648-654, 2018.

[21] T. L. Laber, B. P. Epstein, and M. C. Taylor, "High speed digital video analysis of bloodstain pattern formation from common bloodletting mechanisms," *IABPA News,* pp. 4-12, 2008.

[22] P. M. Comiskey, A. L. Yarin, and D. Attinger, "High-Speed Video Analysis of Forward and Backward Spattered Blood Droplets," *Forensic Science International,* vol. 276, pp. 134-141, 2017.

[23] R. M. Arthur, P. J. Humburg, J. Hoogenboom, M. Baiker, M. C. Taylor, and K. G. de Bruin, "An image-processing methodology for extracting bloodstain pattern features," *Forensic Science International,* vol. 277, pp. 122-132, 2017/08/01/ 2017.

[24] R. M. Arthur, J. Hoogenboom, M. Baiker, M. C. Taylor, and K. G. de Bruin, "An automated approach to the classification of impact spatter and cast-off bloodstain patterns," *Forensic Sci Int,* vol. 289, pp. 310-319, Aug 2018.

[25] T. C. de Castro, M. C. Taylor, D. J. Carr, J. Athens, and J. A. Kieser, "Storage life of whole porcine blood used for bloodstain pattern analysis," *Canadian Society of Forensic Science Journal,* vol. 49, no. 1, pp. 26-37, 2016/01/02 2016.

[26] A. Kolbasov, P. Comiskey, R. P. Sahu, S. Sinha-Ray, A. L. Yarin, B. S. Sikarwar, S. Kim, T. Z. Jubery, and D. Attinger, "Blood Rheology in Shear and Uniaxial Elongation," *Rheologica Acta,* vol. 55, pp. 901-908, 2016.

[27] E. Williams and M. Taylor, "Standardising blood physical properties: Implications for precision bloodstain pattern analysis research " in *IABPA (international association of bloodstain pattern analysts) training conference*, San Diego, CA, 2013.

[28] N. Kabaliuk, M. C. Jermy, E. Williams, T. L. Laber, and M. C. Taylor, "Experimental validation of a numerical model for predicting the trajectory of blood drops in typical crime scene conditions, including droplet deformation and breakup, with a study of the effect of indoor air currents and wind on typical spatter drop trajectories," *Forensic Sci Int,* vol. 245, pp. 107-20, Dec 2014.

[29] N. Laan, K. G. de Bruin, D. Slenter, J. Wilhelm, M. Jermy, and D. Bonn, "Bloodstain Pattern Analysis: implementation of a fluid dynamic model for position determination of victims," *Sci Rep,* Article vol. 5, p. 11461, 2015.

[30] A. Jafari, Y. Xing, C. Moore, A. Donaldson, H. Stone, and D. Attinger, "On Some Fluid Dynamics and Heat Transfer Aspects of Bloodstain Pattern Analysis in Forensics," in *ASME Heat Transfer Conference*, Minneapolis, Minnesota, 2013.

[31] C. Bresteau, S. Guigui, P. Berthier, J. M. Fernandez, and Ieee, "ON THE SECURITY OF AERONAUTICAL DATALINK COMMUNICATIONS: PROBLEMS AND SOLUTIONS," in *2018 Integrated Communications, Navigation, Surveillance Conference*(Integrated Communications Navigation and Surveillance Conference, New York: Ieee, 2018.

[32] M. Grabmuller, P. Cachee, B. Madea, and C. Courts, "How far does it get?--The effect of shooting distance and type of firearm on the simultaneous analysis of DNA and RNA from backspatter recovered from inside and outside surfaces of firearms," (in Eng), *Forensic Sci Int,* Research Support, Non-U.S. Gov't vol. 258, pp. 11-8, Jan 2016.

[33] C. Rossi, L. D. Herold, T. Bevel, L. McCauley, and S. Guadarrama, "Cranial Backspatter Pattern Production Utilizing Human Cadavers," *J Forensic Sci,* vol. 63, no. 5, pp. 1526-1532, Sep 2018.

[34] B. G. Stephens and T. B. Allen, "Back spatter of blood from gunshot wounds. Observations and experimental simulation," *Journal of Forensic Sciences,* vol. 28, no. 2, pp. 437-439, 1983.

[35] P. M. Comiskey, A. L. Yarin, S. Kim, and D. Attinger, "Prediction of blood back spatter from a gunshot in bloodstain pattern analysis," *Physical Review Fluids,* vol. 1, no. 4, p. 043201, 2016.

[36] Anonymous, "literature search for the distance that backspatter travels," *IABPA News,* vol. 23, no. 3, September 2017, pp. 31-32, 2007.

[37] S. H. James, P. E. Kish, and T. P. Sutton, *Principles of Bloodstain Pattern Analysis: Theory and Practice*. CRC Press, 2005.

[38] H. L. MacDonell, *Bloodstain Patterns*, 2nd. ed. Laboratory of Forensic Sciences, Corning, NY USA, 2005.

[39] P. R. D. Forest, R. E. Gaensslen, and H. C. Lee, *Forensic science: An introduction to criminalistics*. McGraw-Hill, New York, 1983.

[40] J. O. Pex and C. H. Vaughan, "Observations of high velocity bloodspatter on adjacent objects," *Journal of Forensic Sciences,* vol. 32, no. 6, pp. 1587-1594, 1987.

[41] B. Karger, R. Nüsse, B. Brinkmann, G. Schroeder, and S. Wüstenbecker, "Backspatter from experimental close-range shots to the head: 1. Macrobackspatter," (in English), *International journal of legal medicine,* vol. 109, no. 2, pp. 66-74, 1996/10/01 1996.

[42] B. Karger, R. Nüsse, H. D. Tröger, and B. Brinkmann, "Backspatter from experimental close-range shots to the head: 2. Microbackspatter and the morphology of bloodstains," *Int J Legal Med (1997) 110 : 27-30,* 1997.

[43] T. Bevel and R. M. Gardner, 2, Ed. *Bloodstain Pattern Analysis with an Introduction to Crime Scene Reconstruction*. CRC Press, Boca Raton, FL, USA, 2002.

[44] J. Bockrath and R. Lugo, "Slugger Slaying Caught on Tape," in *2017 Annual IABPA Training Conference (International Association of Bloodstain Pattern Analysts)*, Crown Plaza Redondo Beach and Marina, 2017.

[45] F. Camana, "Determining the area of convergence in Bloodstain Pattern Analysis: A probabilistic approach," *Forensic Science International,* vol. 231, no. 1-3, pp. 131-136, Sep 10 2013.

[46] T. G. Theofanous, "Aerobreakup of Newtonian and Viscoelastic Liquids," *Annual Review of Fluid Mechanics,* vol. 43, no. 1, pp. 661-690, 2011.

[47] D. Attinger, C. Moore, A. Donaldson, A. Jafari, and H. A. Stone, "Fluid dynamics topics in bloodstain pattern analysis: comparative review and research opportunities," (in eng), *Forensic Sci Int,* vol. 231, no. 1-3, pp. 375-96, 2013.

[48] S. Kim, Y. Ma, P. Agrawal, and D. Attinger, "How important is it to consider target properties and hematocrit in bloodstain pattern analysis?," *Forensic Science International,* vol. 266, pp. 178-184, 2016.

[49] D. Attinger, Y. Liu, R. Faflak, Y. Rao, B. A. Struttman, K. De Brabanter, P. M. Comiskey, and A. L. Yarin, "A data set of bloodstain patterns for teaching and research in bloodstain pattern analysis: gunshot backspatters," submitted to Data in Brief, September 2018.

[50] M. Vargas, "Drag Coefficient of Water Droplets Approaching the Leading Edge of an Airfoil."

[51] E. Loth, "Quasi-steady shape and drag of deformable bubbles and drops," (in English), *International Journal of Multiphase Flow,* Review vol. 34, no. 6, pp. 523-546, Jun 2008.

[52] A. Reinhart, "Das Verhalten fallender Tropfen," *Chem. Ing. Tech.,* p. 36, 1964.

[53] R. Clift, J. R. Grace, and M. E. Weber, *Bubbles, drops and particles*. New York: Academic, 1978.

[54] C. D. Adam, "Fundamental studies of bloodstain formation and characteristics," (in Eng), *Forensic Sci Int,* Jan 5 2012.

[55] R. P. Sahu, S. Sett, A. L. Yarin, and B. Pourdeyhimi, "Impact of aqueous suspension drops onto non-wettable porous membranes: Hydrodynamic focusing and penetration of nanoparticles," *Colloids and Surfaces A: Physicochemical and Engineering Aspects,* vol. 467, pp. 31-45, 2015.

[56] B. L. Scheller and D. W. Bousfield, "Newtonian drop impact with a solid surface," *AICHE Journal,* vol. 41, no. 6, pp. 1357-1367, 1995.

[57] L. P. Hsiang and G. M. Faeth, "DROP PROPERTIES AFTER SECONDARY BREAKUP," *International Journal of Multiphase Flow,* vol. 19, no. 5, pp. 721-735, Oct 1993.

[58] L. P. Hsiang and G. M. Faeth, "DROP DEFORMATION AND BREAKUP DUE TO SHOCK-WAVE AND STEADY DISTURBANCES," *International Journal of Multiphase Flow,* vol. 21, no. 4, pp. 545-560, Aug 1995.

[59] G. Recktenwald, *Numerical methods with Matlab: Implementations and applications*. Upper-Saddle River, NJ.: Prentice-Hall, 2000.